



Laval (Greater Montreal)
June 12 - 15, 2019

EFFECT OF SODIUM OXIDE ON THE PROPERTIES OF ALKALI ACTIVATED SLAG MORTARS

W. Almakhadmeh¹ and A.M. Soliman²

1. PhD student, Department of Building, Civil and Environmental Engineering,

Concordia University, Montreal Quebec Canada

2. Assistant Professor, Department of Building, Civil and Environmental Engineering,

Concordia University, Montreal Quebec Canada

Abstract: Alkali-activated materials (AAMs) are recognized as potential alternatives to ordinary Portland cement (OPC). This study investigated the effect sodium oxide ratio on properties of Alkali Activated Slag mortars (AASm). Shrinkage has a direct impact on its durability, so, in this study, different tests were arranged to examine the effect of sodium oxide ratio (Na₂O) on fresh and hardened properties. In experimental study, three mixes with Na₂O ratios of 4%, 6% and 8% were considered to evaluate workability, setting time, heat of hydration, compressive strength, and drying shrinkage. Generally, the results showed that the 8% Na₂O is the optimum value for AAS mortars mixes from the compressive strength point of view. Based on the results, increasing Na₂O% shortened the setting time, decreased the workability and increased the 28 days' compressive strength. Correspondingly, the drying shrinkage also increase as Na₂O% values increased. This highlighted the importance of controlling the Na₂O% value to achieve adequate strength while maintaining lower shrinkage.

1 INTRODUCTION

Cement manufacturing contributes to about 5 to 7% of the total global greenhouse gas emissions. In 2016, the estimated value was 1.45 ± 0.20 Gt CO₂ (Andrew, 2018). Moreover, the calcination (decarbonation) of limestone at 1400–1450 °C is responsible for around 50–60% of OPC-production-related CO₂ emissions, which cannot be reduced by improving energy efficiency (Damtoft *et al.* 2008). Hence, the need to use eco-friendly construction materials is an urgent need.

Alkali activation technology provides a sustainable alternative binder to Portland cement (Davidovits, 1989). Alkali activated binders are prepared by reacting an alkali source (so called “activator”) and solid aluminosilicate (so called “precursor”). Once, aluminosilicate comes in contact with a high pH alkali activator, different types of amorphous phases are formed, including calcium-silicate-hydrate (C-S-H), calcium-aluminosilicate-hydrate (C-A-S-H), and alkali- alumino-silicate- hydrate (N-A-S-H). Those materials are responsible for the binding characteristics of concrete [Haha *et al.* 2011; Ye and Randiska 2016]. In comparison to ordinary Portland cement (OPC), alkali activated materials (AAMs) have superior properties such as higher resistance to acids and sulfate (Bakharev, 2005), better fire resistance (Sarker *et al.* 2014), and higher compressive strength (up to 130 MPa) (Al Bakri *et al.* 2013). However, long-term durability of AAS concrete, such as rapid carbonation, potential alkali-silica reactivity and the volumetric instability, is still questionable (Thomas *et al.* 2017). Alkali activated slag concrete (AASc) exhibits a large shrinkage and shows a higher risk of cracking. Several studies had investigated the shrinkage behavior of alkali-activated

slag, reporting a high autogenous and drying shrinkage. According to Palacios and Puertas (2007), the shrinkage of two-part AAS mortars activated by sodium silicate can be about 4 times larger than OPC. Researchers stated that AAS pastes and mortars exhibits a viscoelastic/plastic deformation response upon drying at different drying procedures and exposures conditions (Shi *et al.* 2006; Melo Neto *et al.* 2008). Hence, its clear that shrinkage behaviour of AAS and underlying driving forces is still poorly understood and need to be better explained (Douglas *et al.* 1992; Bakharev *et al.* 2000; Palacios and Puertas 2007). Therefore, this study investigates the effect of sodium oxide on the drying shrinkage behavior.

2 MATERIALS AND EXPERIMENTAL WORK

Granulated blast furnace slag (GBFS) was used as the aluminosilicate precursor in all mixtures. Its specific gravity was 2920 kg/m³ and Blaine fineness was 515 m²/kg with an average particle size value was around 14.5 µm. The chemical compositions of GGBFS is shown in Table 1. The basicity coefficient [$K_b = (CaO + MgO)/(SiO_2 + Al_2O_3)$] and the hydration modulus [$(CaO + MgO + Al_2O_3)/SiO_2$] based on the chemical composition were 1.06 and 1.63, respectively. Natural sand with maximum size of 4 mm, water absorption of 3.5% and saturated surface dry density of 2.72 was used. For two-part mixtures, the alkaline activator was prepared by mixing sodium hydroxide (>98% purity) with distilled water and sodium silicate solution. The SiO₂/Na₂O molar ratio of the sodium silicate (SS) was 2.0 with chemical composition of 29.40 wt% SiO₂, 14.70 wt% Na₂O and 55.90 wt% H₂O. The activator solution was prepared 1 day before, and kept at laboratory temperature to allow cooling. Mixtures compositions were adjusted to have different Na₂O contents (i.e. 4%, 6% and 8%) and constant alkali modulus (i.e. 0.5).

Table 1: Chemical compositions of slag.

Items	Percentage (%)
SiO ₂	36.5%
Al ₂ O ₃	10.2%
CaO	37.6%
Fe ₂ O ₃	0.5%
SO ₃	3.1%
MgO	11.8%
K ₂ O	0.4%
Na ₂ O	0.3%
TiO ₂	1%
Manganese Oxide	0.4%

2.1 Test Methods

Two dominant parameters on the reaction kinetics, drying shrinkage and compressive strength are evaluated. Sodium oxide (Na₂O %) range between (4% - 8%) and constant silica modulus (0.5). The water/solid ratio was kept constant (0.4) and the needed water is calculated for each mixture. The solid weight includes the binder weight and the solid weight of activator (NaOH and sodium silicate).

Alkali-activated slag mortars were prepared with sand to binder ratio of 2 for all mixtures. Mixture were prepared by using an electrically driven mechanical mixer conforming to the requirements of ASTM C305. Initially, slag and sand were in a dry state for a minute. The activator solution was dissolved in mixing water and gradually added while mixing continued for about 2 min.

For setting time, alkali-activated slag paste samples were prepared and tested by using Vicat apparatus according to ASTM C191 (standard test method for time of setting of hydraulic cement by Vicat needle). The time of setting was measured on three replicate paste specimens. Compressive strength testing was conducted on 50 mm cubes at the ages 7, and 90 days. Specimens were kept in a humid environment at 22 ± 1 °C and 85 ± 3 % RH, until the testing age. The average of three tested cubes were taken at each age for each mixture.

For shrinkage measurements, eight prismatic specimens $25 \times 25 \times 285$ mm for each mixture were made according to ASTM C 157 (Standard Test Method for Length Change of Hardened Hydraulic-Cement Mortar and Concrete). For total shrinkage measurements were demolded after 24 hours and exposed to dry at the ambient condition of the laboratory (temperature = 20 ± 1 °C and 45 ± 3 % relative humidity). The unrestrained one-dimensional deformations were measured using a comparator provided by a dial gauge with an accuracy of 10 $\mu\text{m/m}$.

Prismatic specimens $25 \times 25 \times 280$ mm were made for measuring mass loss for each mixture. Specimens were demolded at the time of starting total shrinkage measurements. Prisms were transferred to the same exposure condition after measuring the initial mass of each prism using a balance with an accuracy of 0.01 g [0.00035 oz.]. Mass measurements were taken for all prisms along with measurements of total strains. Each mass loss test result in this study represents the average value obtained on four identical prisms (maximum standard deviation of 0.18 g).

3 RESULTS AND DISCUSSION

3.1 Workability

The workability of each mixture was evaluated based on the flow index (F), which is defined as follows (Eq. 1):

$$[1] F (\%) = [(R_{25} - R_0) / R_0] \times 100$$

where R_{25} is the radius of the mortar pile after the 25th drop and R_0 is the initial radius of the mortar pile according to ASTM C 1437 (standard test method for flow of hydraulic cement mortar) [Ref 4].

Fig. 1. Shows the flow values of fresh mortars with different Na_2O values. Based on the results, AAS mortars present less workability by increasing the Na_2O ratios.

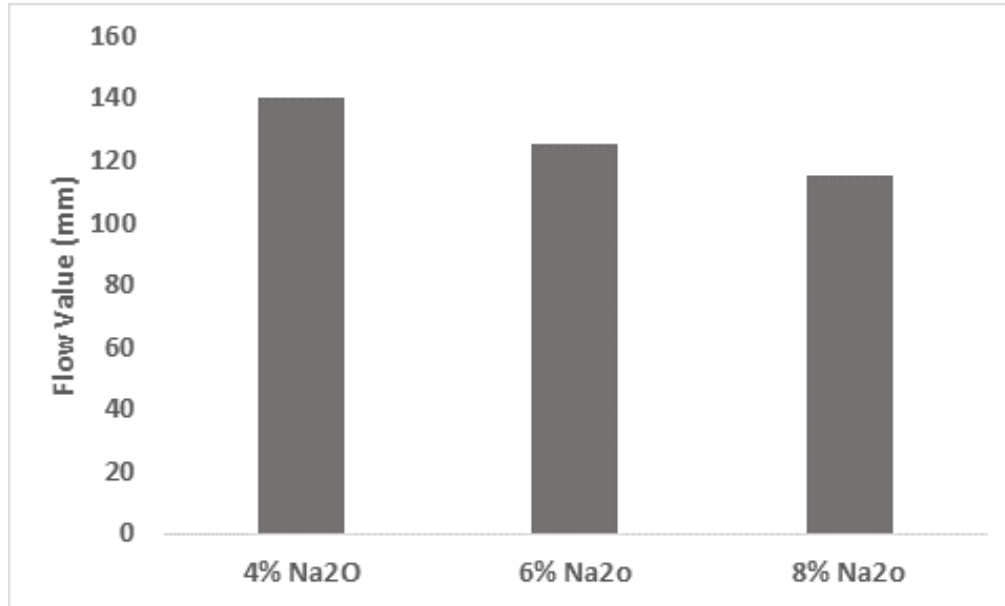


Figure 1: Flow values of AAS mortars.

3.2 Setting time

Initial and final setting times of pastes for various Na₂O values are presented in Table 2. For 4% Na₂O mixture, higher MS ratios caused a slight reduction in the setting times (Fig. 2). For mixtures with 6% and 8% Na₂O contents, setting times of pastes reduced. This quick setting may ascribe to the formation of initial calcium silicate hydrate.

Table 2: Initial and final setting time of pastes.

Mixture	Initial Setting (Min)	Final Setting (Min)
4% Na ₂ O	87	248
6% Na ₂ O	52	105
8% Na ₂ O	22	76

3.3 Compressive Strength and cumulative heat of hydration

Compressive strengths of AAS mortars increased as the dosage of sodium content increased as given in Fig. 2. This can be explained by the pozzolanic reaction. Increasing Na₂O% from 4% to 6% and 8%, intensified the reaction. Correspondingly, as observed the compressive strength increased significantly. As proved by calorimetry analysis, the cumulative heat of hydration is the highest for 8% Na₂O ratio (Fig. 3).

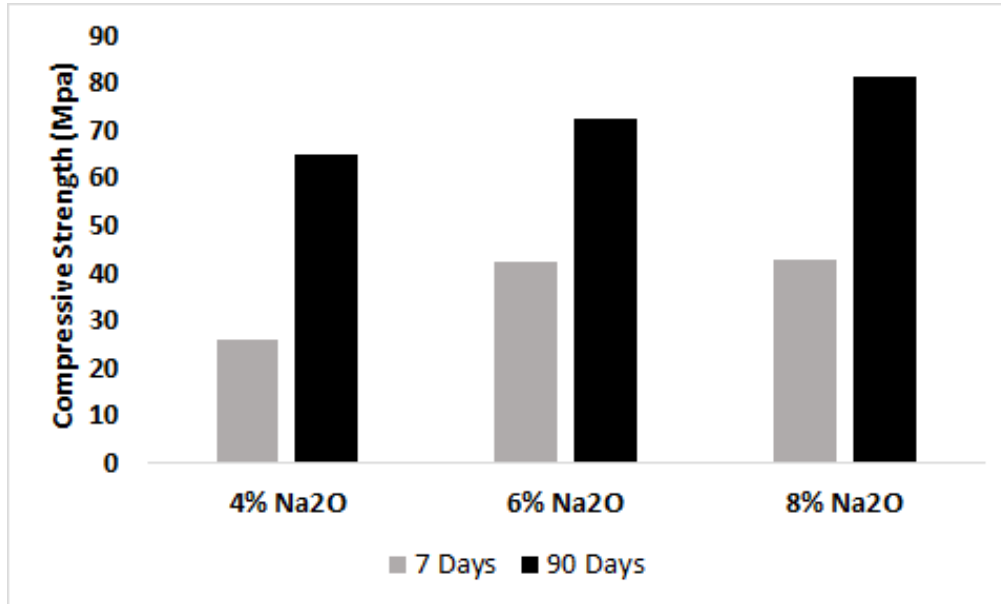


Figure 2: Compressive Strength of AAS mortars at 7 and 90 days' age.

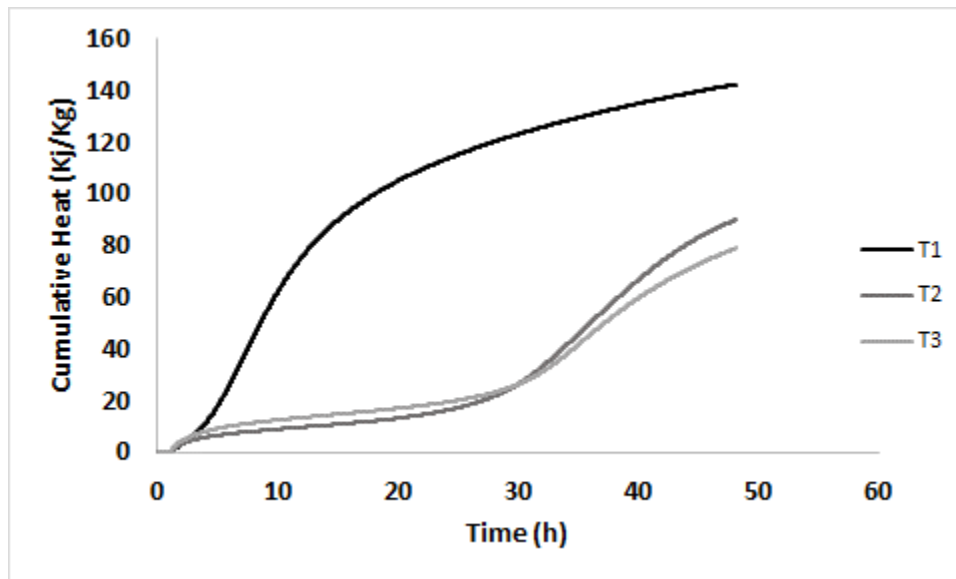


Figure 3: Cumulative heat of hydration for AAS paste

3.4 Drying shrinkage

Drying shrinkage increased with increasing Na₂O content as shown in fig 4. As mentioned above, an increase in activator dosage intensified the degree of hydration, which results in an increase in C–S–H volume and correspondingly, a reduction in porosity. These factors play a crucial role on the principal mechanisms of shrinkage.

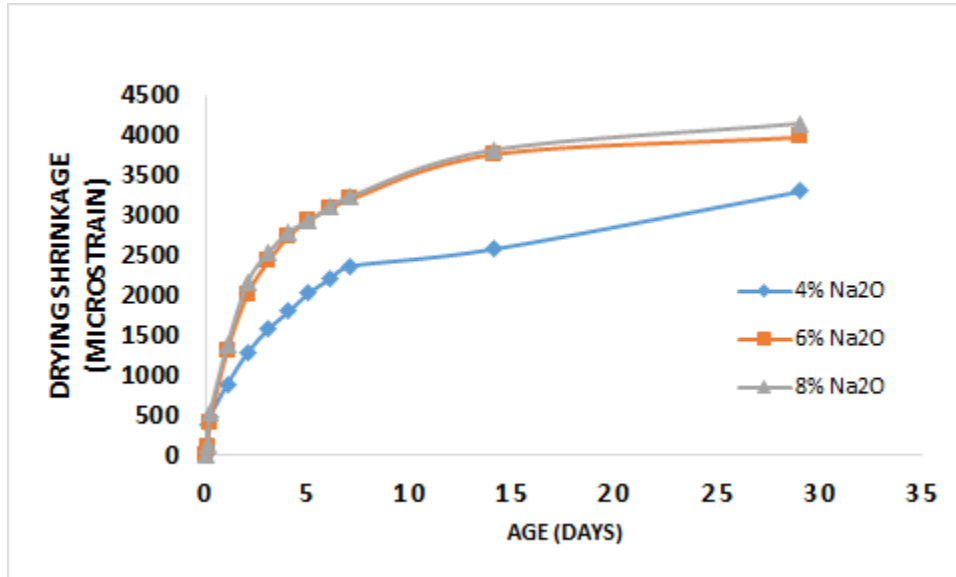


Figure 4: Drying shrinkage values of AAS mortars.

3.5 Mass change characteristic

Under exposure conditions of (22 ± 2) °C and a relative humidity of $(45\pm 2\%)$, the intensity and moment at which water evaporates is highly dependent on the activator content. A higher content of waterglass means less intense loss of water and a shorter period of water loss. As shown in **Fig. 5**, samples from mixture 4% lost water more than samples of 6% Na₂O. While, 8% of Na₂O, released the least water through evaporation. This is attributed to the intensity of the reaction, which means more water was consumed in 8% samples, due to the high alkaline activator dosage and the lower porosity (Neto *et al.* 2007).

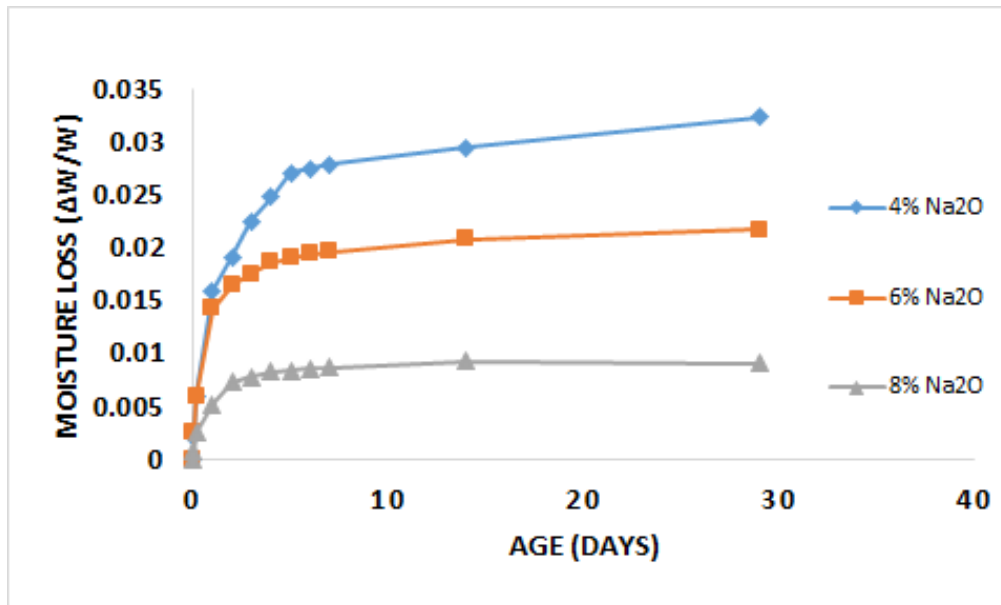


Figure 5: Mass loss for AAS mortars

4 CONCLUSION

The activator dosage plays an important role in the fresh and hardened properties of AAS mortars. Based on the results, higher sodium dosage leads to higher compressive strength and lower workability. Furthermore, AAS mortars experienced a quick setting by increasing the sodium dosage. However, these mixtures are suitable for the works that need quick setting, such as shotcrete. Additionally, drying shrinkage increased by higher dosage, and the water loss by evaporation is not the main reason for the high total shrinkage of ASC. For instance, mixture 4% exhibited the highest drying shrinkage and lowest mass loss. This can be attributed to lower porosity and higher degree of hydration by increasing the dosage.

5 References

- Andrew, R. M. 2018. "Global CO₂ emissions from cement production." *Earth System Science Data* 10 (1):195-217. doi: 10.5194/essd-10-195-2018.
- ASTM C 305-99. Standard practice for mechanical mixing of hydraulic cement pastes and mortars of plastic consistency. In: Annual book of ASTM; 2002.
- ASTM C191. Standard test methods for time of setting of hydraulic cement by vicat needle. Annual Book of ASTM Standards, West Conshohocken, USA; 2005
- Bakharev, T., J. G. Sanjayan, and Y. B. Cheng. 2000. "Effect of admixtures on properties of alkali-activated slag concrete." *Cement and Concrete Research* 30 (9):1367-1374. doi: 10.1016/s0008-8846(00)00349-5.
- Ben Haha, M., G. Le Saout, F. Winnefeld, and B. Lothenbach. 2011. "Influence of activator type on hydration kinetics, hydrate assemblage and microstructural development of alkali activated blast-furnace slags." *Cement and Concrete Research* 41 (3):301-310. doi: 10.1016/j.cemconres.2010.11.016.
- Damtoft, J. S., J. Lukasik, D. Herfort, D. Sorrentino, and E. M. Gartner. 2008. "Sustainable development and climate change initiatives." *Cement and Concrete Research* 38 (2):115-127. doi: 10.1016/j.cemconres.2007.09.008.
- Davidovits, J. 1989. "Geopolymers and geopolymeric materials." *Journal of Thermal Analysis* 35 (2):429-441. doi: 10.1007/bf01904446.
- Douglas, E., A. Bilodeau, and V. M. Malhotra. 1992. "Properties and durability of alkali-activated slag concrete." *Aci Materials Journal* 89 (5):509-516.
- Neto, A. A. M., M. A. Cincotto, and W. Repette. 2008. "Drying and autogenous shrinkage of pastes and mortars with activated slag cement." *Cement and Concrete Research* 38

(4):565-574. doi: 10.1016/j.cemconres.2007.11.002

Palacios, M., and F. Puertas. 2007. "Effect of shrinkage-reducing admixtures on the properties of alkali-activated slag mortars and pastes." *Cement and Concrete Research* 37 (5):691-702. doi: 10.1016/j.cemconres.2006.11.021.

Sarker, P. K., S. Kelly, and Z. T. Yao. 2014. "Effect of fire exposure on cracking, spalling and residual strength of fly ash geopolymer concrete." *Materials & Design* 63:584-592. doi: 10.1016/j.matdes.2014.06.059.

Shi, C. J. 1996. "Strength, pore structure and permeability of alkali-activated slag mortars." *Cement and Concrete Research* 26 (12):1789-1799. doi: 10.1016/s0008-8846(96)00174-3.

Thomas, R. J., D. Lezama, and S. Peethamparan. 2017. "On drying shrinkage in alkali-activated concrete: Improving dimensional stability by aging or heat-curing." *Cement and Concrete Research* 91:13-23. doi: 10.1016/j.cemconres.2016.10.003.

Ye, H. L., and A. Radlinska. 2016. "Shrinkage mechanisms of alkali-activated slag." *Cement and Concrete Research* 88:126-135. doi: 10.1016/j.cemconres.2016.07.001